INFLUENCE OF SONICATION AMPLITUDE ON SURFACE PERFORATION OF CHITOSAN MACROBEADS AND DYE ADSORPTION

Kabilarasan Thanasegaran[1], Swee Pin Yeap[2*], Li Sze Lai[3], Jing Lin Ng[4], Chaomeng Dai[5], Kah Hon Leong[6], Pey Yi Toh[7]

Abstract

Due to industrialisation and globalisation, water sources are increasingly contaminated with dyes. Among the various available methods, adsorption using chitosan macrobeads is a feasible technique for dye removal. However, despite existing studies on the use of chitosan macrobeads for dye adsorption, the influence of controlled surface perforation induced by ultrasonication on their structural integrity and dye adsorption performance has been scarcely reported. Hence, this project aimed to develop chitosan macrobeads with a surface-perforated structure and to investigate how these surface alterations influence their dye adsorption efficiency. Here, chitosan macrobeads were formed using the gelation method and subsequently subjected to high-intensity sonication at various amplitudes (20 %, 40 %, 60 %, 80 %, and 100 %) for 5 minutes to induce surface perforation. As anticipated, significant changes in the surface structure were observed via electron microscopic analysis. In particular, the bead surfaces exhibited wavy and corrugated layers, with the presence of cracks and pores following sonication. Nevertheless, macrobeads treated at higher sonication amplitudes (≥ 60 %) experienced surface rupture, resulting in flake-like layers. Subsequently, dye adsorption studies showed a slight improvement in adsorption efficiency when chitosan macrobeads were sonicated at 40 % amplitude compared to non-sonicated samples. However, a detrimental effect was observed at higher sonication amplitudes (≥ 60 %), where a significant reduction in adsorption efficiency occurred. This study provides insight into the possibility of modifying chitosan macrobeads by imposing intense sonication to generate surface perforations, which subsequently alter their water treatment efficiency.

Received: *29 October, 2025*
Revised: *14 January, 2026*
Accepted: *10 March, 2026*

[1,2,3]Department of Chemical & Petroleum Engineering, Faculty of Engineering, Technology & Built Environment, UCSI University, 56000, Cheras, Kuala Lumpur, Malaysia.

[4]Faculty of Civil Engineering, Universiti Teknologi MARA (UiTM), 40450 Shah Alam, Selangor, Malaysia

[5]College of Civil Engineering, State Key Laboratory of Disaster Reduction in Civil Engineering, Tongji University, 1239 Siping Road, Shanghai 200092, P. R. China.

[6]Department of Civil Engineering, Lee Kong Chian Faculty of Engineering and Science, Universiti Tunku Abdul Rahman 43000, Kajang, Selangor, Malaysia.

[7]Department of Petrochemical Engineering, Faculty of Engineering and Green Technology, Universiti Tunku Abdul Rahman 31900, Kampar, Perak, Malaysia.

****Corresponding author:***
yeapsw@ucsiuniversity.edu.my

DOI: *https://doi.org/10.54552/v87i2.324*

Keywords:
Chitosan bead, Dye pollution, Water treatment, Sonication, Surface perforation

1.0 INTRODUCTION

Adsorption is one of the most widely used approaches for industrial effluent treatment, surpassing other processes such as advanced oxidation and membrane filtration due to its simplicity, technical maturity, high efficiency, and cost-effectiveness (Al-Ghouti *et al.,* 2023; Fouda-Mbanga, Onotu, & Tywabi-Ngeva, 2024). A variety of adsorbents are available for this approach, including activated carbon, zeolites, metal organic frameworks (MOFs), resins, nanomaterials, and biopolymers. Among all adsorbents, activated carbon is well known for its ability to separate a wide range of organic and chemical compounds. Nevertheless, despite its widespread use, the production of activated carbon is costly due to the requirement for high-temperature carbonization (Aulia, Aprilianda, Arsyad, & Johan, 2019; Y. Li *et al.,* 2025) and various chemicals for activation (such as NaOH, H_3PO_4, and Z_nCl_2) (Aulia *et al.,* 2019; Gao, Yue, Gao, & Li, 2020; Muttil, Jagadeesan, Chanda, Duke, & Singh, 2023). These requirements increase the operational costs and environmental burden especially when it comes to large-scale usage. On the other hand, nanoparticles represent a cutting-edge technology with high adsorption efficiency; however, their large-scale application is limited due to recent concerns regarding nano (toxicity) (Frazier *et al.,* 2023; Thu, Haider, Khan, Sohail, & Hussain, 2023). In contrast, biopolymers such as chitosan have gained increasing attention, as they are derived from natural resources, environmentally friendly, and biodegradable. More importantly, chitosan possesses abundant functional groups which include $–NH_2$ and –OH that making it suitable to adsorb

pollutants (Gamage *et al.,* 2023; Hashem & Farag, 2025). In fact, it was recently reported that chitosan has lower carbon footprint (1.5–2.5 kg CO_2-eq/kg) compared to activated carbon (8–12 kg CO_2-eq/kg) (Hashem & Farag, 2025), making it a potential low environmental impact adsorbent.

Chitosan is a linear polysaccharide consists of random copolymer of β-(1→4)-linked D-glucosamine and N-acetyl-D-glucosamine (Qiu, Hamilton, & Temenoff, 2011). This biopolymer is normally produced through the deacetylation of chitin (Aranaz *et al.,* 2021), which is extracted from natural sources such as the exoskeletons of crustaceans and insects (Ngasotter *et al.,* 2023), the gladius of squid (Kim, Song, Kim, Kim, & Jin, 2024), the cuttlebone of cuttlefish (Hazeena *et al.,* 2022), and the cell walls of fungi (Huq *et al.,* 2022). Despite its common use as a flocculant in water treatment, chitosan is also a promising adsorbent due to its unique functional groups, namely, amino and hydroxyl groups, which facilitate interactions or chelation with both organic and inorganic pollutants (Dago-Serry, Maroulas, Tolkou, Kokkinos, & Kyzas, 2024; Rostami & Khodaei, 2024). For instance, it was recently reported that both chitosan powder and chitosan bead are effective at adsorbing Direct Blue 78 dye from aqueous solution, with maximum adsorption capacities of 10.5 mg/g and 26.3 mg/g, respectively (Elzahar & Bassyouni, 2023). The adsorption was governed by electrostatic attraction between the positively charged chitosan molecules and the negatively charged dye molecules. Meanwhile, chitosan also able to form complexes (via chelate) with various transition metal ions and heavy metal ions include Cu^{2+}, Ni^{2+} and Hg^{2+} (Firnanelty, Chadijah, Ratna, Nurhuda, & Sittiama, 2021). In fact, chitosan can be manufactured into different structural forms include hydrogels, beads, membranes, fibres, films, and aerogels, which give more rooms to improve its adsorption capacity (Dago-Serry *et al.,* 2024; Kuang *et al.,* 2023; Rostami & Khodaei, 2023).

While the use of dissolved chitosan as a flocculant for water treatment has been reported for decades, it often results in the formation of sludge (Guibal & Roussy, 2007; Guibal, Touraud, & Roussy, 2005; Sanghi & Bhattacharya, 2005). In contrast, employing chitosan in solid forms as an adsorbent (e.g., beads) enables pollutant removal through adsorption without producing sludge. The solid form of chitosan is typically produced through physical gelation (Li, Qin, Xue, Lin, & Jiang, 2025; Lu, Zou, Zhou, Huang, & Zhang, 2022) or through chemical crosslinking with agents such as glutaraldehyde and epichlorohydrin (Beppu, Vieira, Aimoli, & Santana, 2007; Sapuła, Bialik-Wąs, & Malarz, 2023; Xiao, Shan, & Wu, 2023). For instance, our recent work demonstrated that chitosan macrobeads were able to remove over 90% of green algae from pond water, leaving a clear solution; in contrast, flocculating the green algae with dissolved chitosan resulted in a cloudy solution, indicating the presence of sludge (Thanasegaran, Yeap, Lai, & Wong, 2023). Research has been ongoing to further modify this biopolymer in order to enhance its adsorption efficiency (Upadhyay, Alimohammadi, & Tehrani, 2024). For instance, a recent study by Rodrigues *et al.* (2025) showed that pre-treatment of chitosan films with ethanol (immersion for 24 hours) and NaOH (immersion for 2 seconds) significantly improved mechanical stability and doubled the adsorption capacity (Rodrigues, Lopes, Longhinotti, & Diógenes, 2025). Despite existing studies on the use of chitosan macrobeads for dye adsorption, the influence of controlled surface perforation induced by ultrasonication on their structural integrity and dye adsorption performance has been scarcely reported. To close this research gap, in the present work, chitosan macrobeads were produced via gelation and subsequently treated with various ultrasonication conditions to induce surface perforation. Subsequently, the ultrasonicated chitosan macrobeads were characterised to assess changes in surface structure and functionality prior to their application in dye removal. It was hypothesised that the formation of pores on the bead surface would provide additional adsorption sites, thereby improving the overall adsorption efficiency.

2.0 METHODOLOGY

2.1 Materials

The materials used in this study included chitosan with a molecular weight of 30,000–190,000 g/mol (Sigma-Aldrich), acetic acid (AcOH) with a purity of 99.8–100.5% (Sigma-Aldrich), sodium hydroxide (NaOH) (Chemiz (M) Sdn. Bhd.), and methyl orange (MO) (Chemiz (M) Sdn. Bhd.). All chemicals were used as received without further purification or modification.

2.2 Synthesis of Chitosan Macrobead

The preparation of the adsorbent was referred to the previous research works (Thanasegaran *et al.,* 2023) and (Wong, Tay, & Lim, 2020). Firstly, 2 g of chitosan powder was dissolved in 100 mL of 1% (v/v) AcOH solution to prepare a chitosan stock solution. The mixture was magnetically stirred at 400 rpm for 24 hours to ensure complete dissolution. Meanwhile, a 10 M NaOH solution was prepared by dissolving 40 g of NaOH pellets in 100 mL of distilled water. The chitosan stock solution was then carefully added dropwise into the NaOH solution using a dropper, resulting in the formation of chitosan macrobeads. To ensure uniform macrobead size, the same dropper was used throughout the synthesis, and droplets were released at approximately the same rate. During this process, the NaOH solution was gently stirred at 125 rpm to prevent the stacking of the macrobeads. The formed chitosan macrobeads were allowed to stand for 24 hours to enhance their structural rigidity. Finally, the macrobeads were thoroughly rinsed with distilled water to remove any residual reactants before being used in subsequent studies. Note that the average size of the macrobeads is around 30 mm, as reported in our previous work (Thanasegaran *et al.,* 2023).

2.3 Preparation of Sonicated Chitosan Macrobeads

Sonicated macrobeads were prepared using a similar procedure to that described in Section 2.1, with the exception that the formed chitosan macrobeads were subjected to high-intensity sonication at varying amplitudes (20%, 40%, 60%, 80%, and 100%) for 5 minutes using an ultrasonic processor (Hielscher UP200s), prior to rinsing with distilled water. The sonication amplitude was varied to induce different levels of surface perforation on the chitosan macrobeads. Figure 1

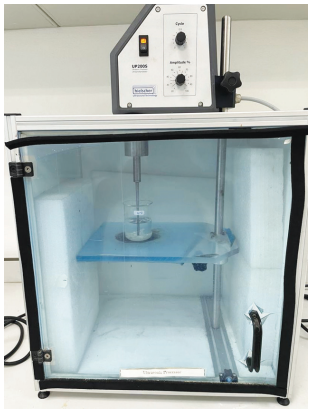

Figure 1: The setup of the probe sonicator for surface perforation of chitosan macrobeads. The probe tip was immersed in the solution up to 1 cm above the bottom of the beaker

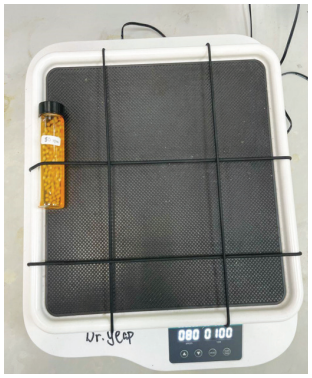

Figure 2: The conduct of MO adsorption study on an orbital shaker

shows the experiment setup for this section. The sonicated chitosan macrobeads were stored in distilled water and used for dye adsorption experiments within one month. Prior to adsorption, excess surface moisture was gently removed by carefully tapping the beads with tissue paper.

2.4 Characterise Structure Morphology and Functional Group of the Chitosan Macrobeads

The surface morphology and functional groups of the synthesized samples were analysed using a Scanning Electron Microscope (SEM, Tescan VEGA3) and Fourier Transform Infrared Spectroscopy (FTIR, PerkinElmer Spectrum Two), respectively. A series of SEM images were captured at various magnifications. Prior to analysis, all samples were sputter-coated with platinum. This characterisation was performed on six samples: chitosan macrobeads and chitosan macrobeads sonicated at amplitudes of 20% to 100%, in order to observe changes in size and surface morphology. Meanwhile, FTIR was used to identify changes in surface functional groups resulting from the sonication treatment at varying amplitudes.

2.5 Dye Adsorption Test

A stock solution of MO at a concentration of 1000 mg/L was prepared by dissolving 1000 mg of the dye in 1 L of distilled water. This stock solution was subsequently diluted to obtain the desired concentrations for experimental use. The concentration of the MO solution was determined using a UV-Vis spectrophotometer (Biobase BK-UV1800PC) operating in absorbance wavelength of 468 nm. A calibration curve was constructed at this wavelength using MO concentrations ranging from 10 to 70 mg/L, correlating absorbance values with dye concentration.

The adsorption test was conducted to investigate the effect of sonication amplitude on dye removal efficiency using 10 g of as-prepared chitosan macrobeads treated at different amplitudes (0 %, 20 %, 40 %, 60 %, 80 %, and 100 %). Each type of macrobeads was placed in a glass bottle containing 20 mL of a 50 mg/L MO dye solution to initiate the adsorption process. The bottles were then placed on an orbital shaker (Joanlab OS-20) operating at 200 rpm, as illustrated in Figure 2. After 3 hours of shaking, the adsorption process was terminated, and the final dye solution was transferred into a cuvette for absorbance measurement. The adsorption efficiency was calculated using Equation 1.

$$R\,(\%) = \frac{C_o - C_e}{C_o} \times 100\% \qquad \text{(Eqn. 1)}$$

Where, C_o and C_e represent the initial and final concentrations of the dye solution (mg/L) respectively, while R is the removal efficiency.

3.0 RESULTS AND DISCUSSION

3.1 Changes in Surface Morphology of the Chitosan Macrobeads

The surface morphology of the as-prepared chitosan macrobeads was examined using SEM, and the results are shown in Figure 3. As illustrated in Figure 3, the incorporation of sonication altered the surface structure of the macrobeads by transforming the initially smooth surface (Figure 3a) into a rougher texture (Figure 3b-f). By taking a closer look at the surface structure of the sonicated chitosan macrobeads at higher magnification (5000×), it was found that the bead surface exhibits wavy and corrugated layers with the presence of cracks and pores. Furthermore, chitosan macrobeads treated at higher sonication amplitudes of 60 %, 80 %, and 100 % were noticed to have ruptured into flake-like layers. Apparently, the application of sonication has imposed intense physical forces that disrupting the internal bonding network (hydrogen bonds) of the chitosan macrobeads (Jamalabadi, Saremnezhad, Bahrami, & Jafari, 2019; Khoerunnisa *et al.,* 2021), leading to the rupture of the bead surface into flake-like structure.

The direct contact of the sonication probe with the beads serves as another reason leading to such a broken structure. Accordingly, the present study has successfully modified the surface morphology of the macrobeads by varying the sonication amplitude. It is envisaged that the formation of pores and cracks will increase the available active sites for pollutant adsorption (Ang *et al.,* 2024).

Figure 4 depicts digital photographs of the chitosan macrobead solutions after sonication treatment. Notably, the cloudiness of the water changes with the sonication amplitude, with samples treated at higher amplitudes (e.g., 80% and 100%) appearing cloudier. The water turns cloudy due to a higher amount of disintegrated chitosan suspended in it.

3.2 Changes in Surface Functional Groups of the Chitosan Macrobeads

Figure 5 shows the FTIR spectra of both unsonicated and sonicated chitosan macrobeads, scanned across the wavenumber range of 4000 cm^{-1} to 400 cm^{-1}, to examine differences in their functional groups. Table 1 presents the corresponding functional groups associated with each significant peak observed in the spectra. Overall, all the beads exhibit peaks at similar wavenumber ranges, including a signal at 896 cm^{-1}, which corresponds to the C–H bending out of the plane of the monosaccharide ring (Fernandes

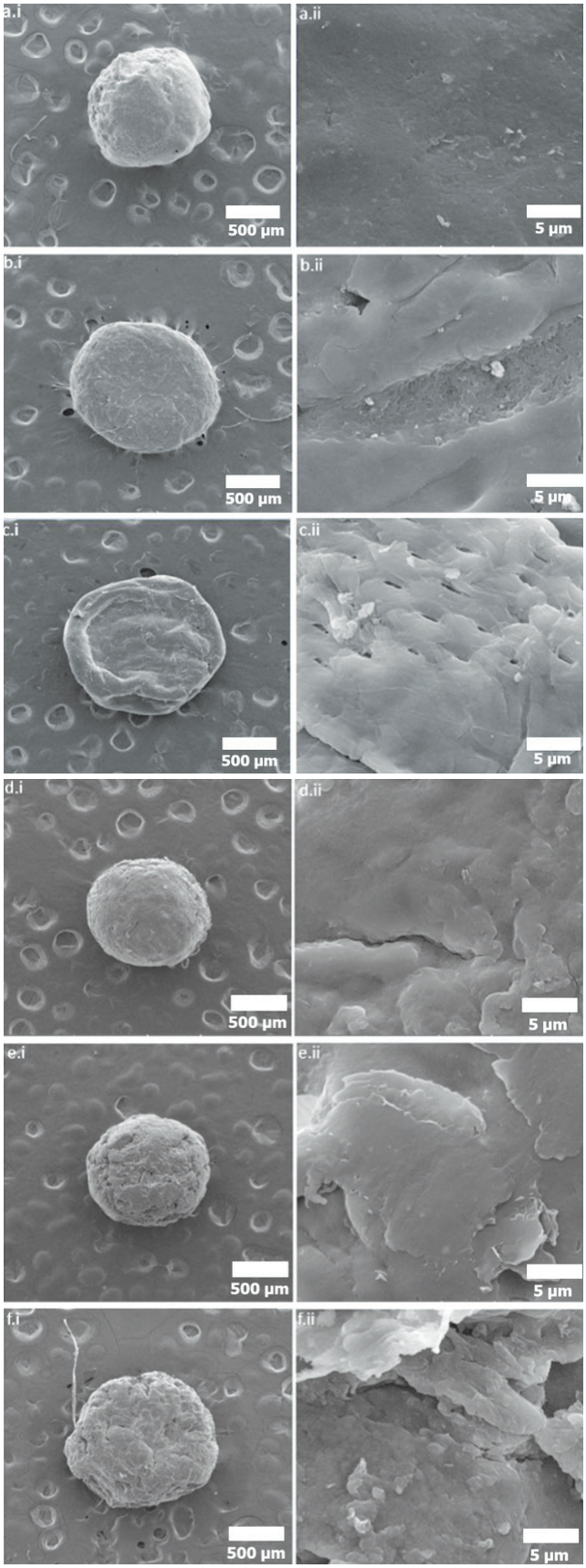

Figure 3: SEM images of chitosan macrobead obtained at 50x (left) and 5000x (right) magnifications. The chitosan macrobeads were sonicated at (a) 0 %, (b) 20 %, (c) 40 %, (d) 60 %, (e) 80 %, and (f) 100 % for 5 mins

Queiroz, Melo, Sabry, Sassaki, & Rocha, 2015). Meanwhile, the pronounced peak observed between 1029.87 cm^{-1} and 1079.79 cm^{-1} is attributed to the stretching vibrations of the C–O bonds (Dissanayake, Pathirana, Wanasekara, Mahltig, & Nandasiri, 2023). In addition, the C-O-C bridge's asymmetric stretching is responsible for the absorption band at 1149.33 cm^{-1} (Dissanayake *et al.,* 2023). The small signal around 1251.78 cm^{-1} corresponded to the bending vibrations of OH present in chitosan (Fernandes Queiroz *et al.,* 2015).

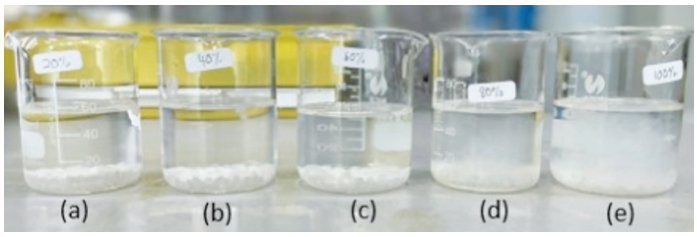

Figure 4: Digital photographs showing the changes in water cloudiness after the chitosan macrobeads being sonicated using (a) 20 %, (b) 40 %, (c) 60 %, (d) 80 %, and (e) 100 % of sonication amplitude

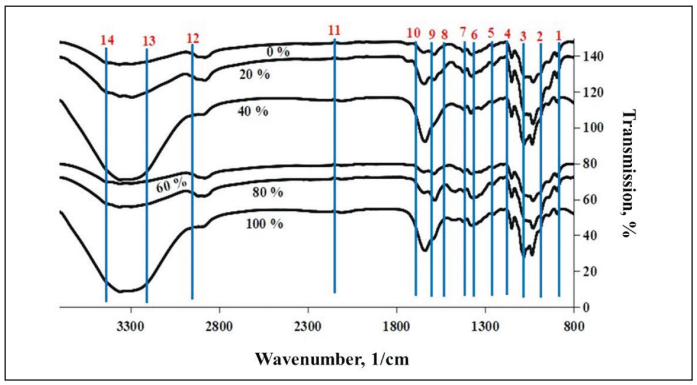

Figure 5: FTIR spectra of the unsonicated and sonicated chitosan macrobeads

Table 1: Legend for FTIR spectra shown in Figure 5

No.	Wavenumber (cm^{-1})	Functional Group	References
1	893.54	• C-H stretching	(Fernandes Queiroz *et al.,* 2015)
2-3	1029.87 - 1079.79	• C-O stretching	(Dissanayake *et al.,* 2023)
3-4	1149.33	• C-O-C	(Dissanayake *et al.,* 2023)
5	1251.78	• OH	(Fernandes Queiroz *et al.,* 2015)
6-7	1375.78 - 1420.55	• CH_2 bending and CH_3 deformation	(Moosa, Ridha, & Kadhim, 2016)
8-9	1584.08 - 1588.24	• N-H stretching	(Dissanayake *et al.,* 2023)
9-10	1645.75	• C=O in the $NHCOCH_3$ group	(Chung & Ong, 2021; Dissanayake *et al.,* 2023)
11-12	2800 - ~2900	• C-H symmetric and asymmetric stretching	(Fernandes Queiroz *et al.,* 2015)
13-14	3291.52 - 3362.48	• O-H stretching vibrations. • N-H stretching vibrations	(Chung & Ong, 2021)

The bending vibration of N-H cause the absorptions between 1584.08 cm^{-1} and 1588.24 cm^{-1} (Dissanayake *et al.,* 2023). The presence of residual acetyl groups is evidenced by the bands at approximately 1645.75 cm^{-1} (C=O stretching of amide I) (Chung & Ong, 2021; Dissanayake *et al.,* 2023). The absorption bands at ~2800 cm^{-1} and ~2900 cm^{-1} can be assigned to C-H symmetric and asymmetric stretching, correspondingly (Fernandes Queiroz *et al.,* 2015). As shown in the FTIR spectrum of chitosan macrobeads, a strong absorption band from 3291 cm^{-1} to 3362 cm^{-1} was attributed to the overlapped stretching vibration of –OH and N–H (Chung & Ong, 2021). Note that there is no clear trend on the intensity of the absorption band from 3291 cm^{-1} to 3362 cm^{-1}, which is likely due to non-uniform water retention in the beads arising in the sample drying stage prior to FTIR analysis. Despite that, regardless of the sonication amplitude, the FTIR spectra of the chitosan macrobeads appear to be the same. Such observation suggested that the application of sonication does not alter the key functional groups of the chitosan macrobeads. Notably, the band at 1645.75 cm^{-1} shows increased intensity in the sonicated beads relative to the unsonicated ones, likely due to the exposure of internal functional groups resulting from surface exfoliation.

3.3 Unsonicated and Sonicated Chitosan Macrobeads for Dye Adsorption

Next, the as-prepared chitosan macrobeads were used for adsorption of MO. In this regard, the adsorption of MO onto the chitosan macrobeads is primarily governed by electrostatic attraction, as the dye is anionic due to sulfonate groups (Wu *et al.,* 2021) and chitosan is cationic due to protonated – NH_2 groups under acidic to ~ pH 6.38 (point of zero charge) conditions (Munim, Saddique, Raza, & Majeed, 2018). The effects of varying the sonication amplitude from 0 % to 100 % on chitosan macrobeads and its subsequent impact on MO adsorption efficiency were investigated. As depicted in Figure 6, chitosan macrobeads treated with sonication amplitudes of 0 %, 20 %, 40 %, 60 %, 80 %, and 100 % exhibited adsorption removal efficiencies of 40 %, 41 %, 42 %, 31 %, 30 %, and 29 %, respectively. This result demonstrates that the sonication amplitude does have a considerable impact on the removal effectiveness. By taking a closer look at the experimental standard deviation and significance of the study, it was found that there is no significant difference in the adsorption efficiencies of chitosan macrobeads produced at 0 %, 20 %, and 40 % efficiency despite the average value showed a slight increment from 40 % to 42 %. The slight increase can be attributed to surface perforation induced by sonication, which creates additional adsorption sites (as shown in Figure 3a-c).

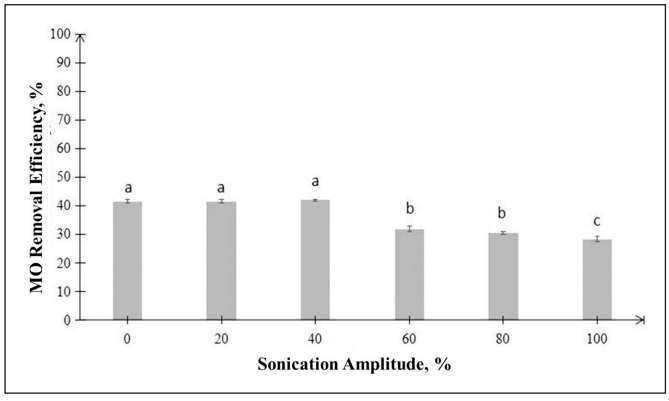

Figure 6: MO removal efficiency using the unsonicated and sonicated chitosan macrobeads. Experimental conditions: 50 mg/L MO solution, pH 5, 20 mL total dye volume, 8 g chitosan macrobeads, agitation speed of 200 rpm, and contact time of 3 hours.

**statistically significant difference determined by t-test (P < 0.05)*

Nevertheless, chitosan macrobeads treated with higher sonication amplitudes (ranging from 60 % to 100 %) exhibited a reduction in adsorption efficiency. This outcome can be attributed to the breaking of chitosan macrobeads under the intense cavitation-induced mechanical stresses exerted during sonication. As presented in Figure 3d–f, the surface of the chitosan macrobeads ruptured into small flake-like structures rather than forming pores. Furthermore, some of these small structures disintegrated from beads and remained suspended in the water, appearing as a cloudy solution as shown in Figure 4c–d. These disintegrated fragments caused the beads to be less solidified and lack surface integrity, resulting in reduced MO adsorption performance. Apparently, a stable and well-formed bead is essential for effective adsorption applications.

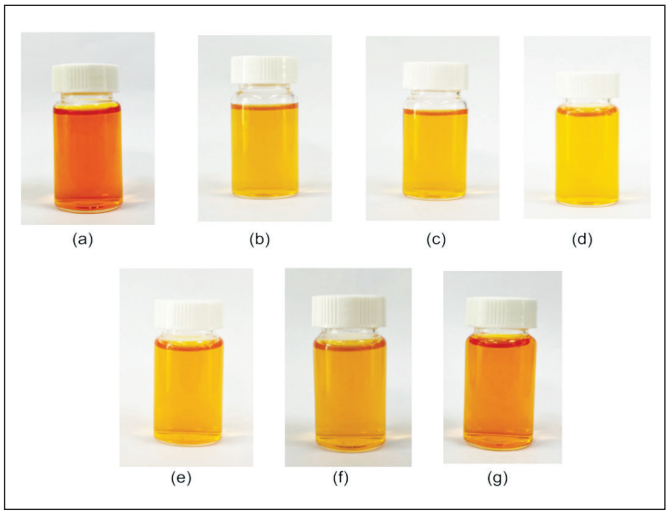

Figure 7: Digital images showing the appearance of the a) initial MO solution (50 mg/l), and remaining solution after adsorbed by chitosan macrobeads prepared at sonication amplitude of b) 0 %, c) 20 %, d) 40 %, e) 60 %, f) 80 %, and g) 100 %

Figure 7 shows the digital image of the leftover solution of MO molecules after the adsorption process, a darker orange colour in samples Figure 7f and Figure 7g indicated the adsorption process was less successful, rendering a higher MO concentration in the remaining solution. This result contrasts with (Low, Tan, Chin, & Tan, 2018), who reported that peanut husk powder sonicated with the same probe sonicator at 60 % amplitude exhibited more surface pores and higher adsorption efficiency than the unsonicated counterpart. Such deviation could be ascribed to the less resilience of the chitosan macrobeads towards cavitation-induced mechanical stresses as compared to peanut husk powder.

4.0 CONCLUSION

The present work revealed that modification of chitosan macrobeads can be achieved through the application of intense ultrasonication. Electron microscopic analysis showed that chitosan macrobeads sonicated at amplitudes of 20 % – 40 % exhibited wavy and corrugated surfaces, along with the formation of cracks and pores. However, increasing the sonication amplitude to 60 % – 100 % resulted in fragmentation of the bead surface into flake-like structures. In fact, under such high sonication amplitudes, some fragments of the beads have disintegrated and became suspended in the solution, causing the initially clear water to turn turbid. FTIR analysis showed that key functional groups of chitosan, including –OH, C=O and N–H bonds, were retained in the sonicated counterparts. In terms of dye adsorption efficiency, the unsonicated chitosan macrobeads were able to remove 40 % of MO after 3 hours of batch adsorption. Only a slight increase in adsorption efficiency was observed when the chitosan macrobeads were moderately sonicated; the slight increase is attributed to sonication-induced surface perforation, creating additional adsorption sites.

However, a significant reduction in adsorption efficiency was observed when the chitosan macrobeads were sonicated at amplitudes ≥ 60 %, as supported by SEM analysis showing that the bead surfaces had fragmented into flake-like structures, with portions of them have disintegrated from the beads. In overall, this study has demonstrated that controlled ultrasonication is a feasible method to tailor the surface structure of chitosan macrobeads, thereby offering insights for modifying chitosan-based adsorbents for effective water treatment applications. For future studies, further optimization of the sonication-induced surface perforation should be carried out by manipulating other sonication conditions which include sonication time and temperature. The macrobead structure can be further characterised for crystallinity via X-ray Diffraction and surface area using Brunauer–Emmett–Teller analyser. In addition, the dye desorption and reusability of the chitosan macrobeads in dye adsorption applications should be investigated. ■

ACKNOWLEDGEMENT

This authors thanks UCSI University for providing facilities and resources for completion of this project.

AUTHORS' CONTRIBUTIONS

Kabilarasan Thanasegaran	Methodology, Formal analysis, Investigation, Writing - Original Draft.
Swee Pin Yeap	Conceptualisation, Visualisation, Supervision, Resources, Funding acquisition, Validation, Writing - Review & Editing.
Li Sze Lai	Conceptualisation, Resources, Writing - Review & Editing.
Jing Lin Ng	Conceptualisation, Investigation, Visualisation.
Chaomeng Dai	Visualisation, Conceptualisation.
Kah Hon Leong	Visualisation, Conceptualisation.
Pey Yi Toh	Conceptualisation, Resources, Visualisation.

REFERENCES

[1] Al-Ghouti, M. A., Ashfaq, M. Y., Khan, M., Al Disi, Z., Da'na, D. A., & Shoshaa, R. (2023). State-of-the-art adsorption and adsorptive filtration based technologies for the removal of trace elements: A critical review. *Science of The Total Environment,* 895, 164854. doi: https://doi.org/10.1016/j.scitotenv.2023.164854

[2] Ang, Y., Kabilarasan, T., Teo, S. S., Lim, L. H., Su, S. F., Mangnomek, V., Yeap, S. P. (2024). Ultrasound treatment of chitosan macrobeads for crack formation and application in column dynamics sorption of methyl orange. *International Journal of Environmental Science and Technology*. https://doi.org/10.1007/s13762-024-06236-w

[3] Aranaz, I., Alcántara, A. R., Civera, M. C., Arias, C., Elorza, B., Heras Caballero, A., & Acosta, N. (2021). Chitosan: An overview of its properties and applications. Polymers, 13(19), 3256. https://doi.org/10.3390/polym13193256

[4] Aulia, Aprilianda, Arsyad, F. S., & Johan, A. (2019). Temperature carbonization effect on the quality of activated carbon based on rubber seed shell. *Journal of Physics: Conference Series,* 1282(1), 012043. https://doi.org/10.1088/1742-6596/1282/1/012043

[5] Beppu, M. M., Vieira, R. S., Aimoli, C. G., & Santana, C. C. (2007). Crosslinking of chitosan membranes using glutaraldehyde: Effect on ion permeability and water absorption. *Journal of Membrane Science,* 301(1), 126-130. doi: https://doi.org/10.1016/j.memsci.2007.06.015

[6] Chung, W.-Y., & Ong, S.-T. (2021). Effective removal of reactive brown 10 from aqueous solution by using chitosan beads: batch and experimental design studies. *Journal of Physical Science,* 32(1), 91-108.

[7] Dago-Serry, Y., Maroulas, K. N., Tolkou, A. K., Kokkinos, N. C., & Kyzas, G. Z. (2024). How the chitosan structure can affect the adsorption of pharmaceuticals from wastewaters: An overview. *Carbohydrate Polymer Technologies and Applications,* 7, 100466. https://doi.org/10.1016/j.carpta.2024.100466

[8] Dissanayake, N. S. L., Pathirana, M. A., Wanasekara, N. D., Mahltig, B., & Nandasiri, G. K. (2023). Removal of methylene blue and congo red using a chitosan–graphene oxide-electrosprayed functionalized polymeric nanofiber membrane. *Nanomaterials,* 13(8), 1350.

[9] Elzahar, M. M. H., & Bassyouni, M. (2023). Removal of direct dyes from wastewater using chitosan and polyacrylamide blends. *Scientific Reports,* 13(1), 15750. https://doi.org/10.1038/s41598-023-42960-y

[10] Fernandes Queiroz, M., Melo, K. R. T., Sabry, D. A., Sassaki, G. L., & Rocha, H. A. O. (2015). Does the use of chitosan contribute to oxalate kidney stone formation? *Marine Drugs,* 13(1), 141-158.https://doi.org/10.3390/md13010141

[11] Firnanelty, Chadijah, S., Ratna, Nurhuda, S., & Sittiama. (2021). Synthesis of chitosan-CuO composite and it's application as heavy metal adsorbent. *Journal of Physics: Conference Series,* 1899(1), 012029. https:// doi.org/10.1088/1742- 6596/1899/1/012029

[12] Fouda-Mbanga, B. G., Onotu, O. P., & Tywabi-Ngeva, Z. (2024). Advantages of the reuse of spent adsorbents and potential applications in environmental remediation: A review. *Green Analytical Chemistry,* 11, 100156. doi: https://doi.org/10.1016/j.greeac.2024.100156

[13] Frazier, E. A., Patil, R. P., Mane, C. B., Sanaei, D., Asiri, F., Seo, S. S., & Sharifan, H. (2023). Environmental exposure and nanotoxicity of titanium dioxide nanoparticles in irrigation water with the flavonoid luteolin. RSC Advances, 13(21), 14110-14118. https:// doi.org/10.1039/d3ra01712e

[14] Gamage, A., Jayasinghe, N., Thiviya, P., Wasana, M. L. D., Merah, O., Madhujith, T., & Koduru, J. R. (2023). Recent application prospects of chitosan based composites for the metal contaminated wastewater treatment. *Polymers*, 15(6), 1453.

[15] Gao, Y., Yue, Q., Gao, B., & Li, A. (2020). Insight into activated carbon from different kinds of chemical activating agents: A review. *Science of The Total Environment,* 746, 141094. https://doi.org/10.1016/j.scitotenv.2020.141094

[16] Guibal, E., & Roussy, J. (2007). Coagulation and flocculation of dye-containing solutions using a biopolymer (Chitosan). *Reactive and Functional Polymers,* 67(1), 33-42.https://doi.org/10.1016/j.reactfunctpolym.2006.08.008

[17] Guibal, E., Touraud, E., & Roussy, J. (2005). Chitosan interactions with metal ions and dyes: dissolved-state vs. solid-state application. *World Journal of Microbiology and Biotechnology,* 21(6), 913-920. https://doi.org/10.1007/ s11274-004-6559-5

[18] Hashem, A., & Farag, S. (2025). Chitosan-based adsorbents for water purification: Mechanisms, performance, and sustainability. *Applied Surface Science Advances,* 30, 100804. https://doi.org/10.1016/j. apsadv.2025.100804

[19] Hazeena, S. H., Hou, C.-Y., Zeng, J.-H., Li, B.-H., Lin, T.-C., Liu, C.-S., Shih, M.-K. (2022). Extraction optimization and structural characteristics of chitosan from Cuttlefish (S. pharaonis sp.) bone. *Materials,* 15(22), 7969.

[20] Huq, T., Khan, A., Brown, D., Dhayagude, N., He, Z., & Ni, Y. (2022). Sources, production and commercial applications of fungal chitosan: A review. *Journal of Bioresources and Bioproducts,* 7(2), 85-98. https:// doi. org/10.1016/j.jobab.2022.01.002

[21] Jamalabadi, M., Saremnezhad, S., Bahrami, A., & Jafari, S. M. (2019). The influence of bath and probe sonication on the physicochemical and microstructural properties of wheat starch. *Food Science & Nutrition,* 7(7), 2427-2435. https://doi.org/10.1002/fsn3.1111

[22] Khoerunnisa, F., Yolanda, Y. D., Nurhayati, M., Zahra, F., Nasir, M., Opaprakasit, P., & Ng, E.-P. (2021). Ultrasonic synthesis of nanochitosan and its size effects on turbidity removal and dealkalization in wastewater treatment. *Inventions,* 6(4), 98.

[23] Kim, J.-K., Song, M.-O., Kim, J., Kim, S., & Jin, J. (2024). Cryomilling-assisted high purity β-chitin extraction from Uroteuthis edulis pens. *International Journal of Biological Macromolecules,* 268, 131815. https://doi. org/10.1016/j. ijbiomac.2024.131815

[24] Kuang, J., Cai, T., Dai, J., Yao, L., Liu, F., Liu, Y., Peng, H. (2023). High strength chitin/chitosan-based aerogel with 3D hierarchically macro-meso-microporous structure for high-efficiency adsorption of Cu(II) ions and Congo red. *International Journal of Biological Macromolecules,* 230, 123238. https://doi. org/10.1016/j.ijbiomac.2023.123238

[25] Li, Y., Yan, X., Cui, Z., Yuan, J., Xu, B., & Yang, G. (2025). Design and preparation of activated carbon with high specific surface area and porosity through an organic activator coupled with co2 activation. *Advanced Materials Interfaces,* 12(3), 2400450. https://doi.org/10.1002/ admi.202400450

[26] Li, Z., Qin, R., Xue, J., Lin, C., & Jiang, L. (2025). Chitosan-based hydrogel beads: developments, applications, and challenges. *Polymers,* 17(7), 920.

[27] Low, S. K., Tan, M. C., Chin, N. L., & Tan, K. W. (2018). Comparative studies on ultrasound pre-treated peanut husk powder and ultrasound simultaneous process on heavy metal adsorption. *International Journal of Engineering,* 31(8), 1334-1340.

[28] Lu, Z., Zou, L., Zhou, X., Huang, D., & Zhang, Y. (2022). High strength chitosan hydrogels prepared from NaOH/ urea aqueous solutions: the role of thermal gelling. *Carbohydrate Polymers,* 297, 120054. https://doi. org/10.1016/j.carbpol.2022.120054

[29] Moosa, A., Ridha, A., & Kadhim, N. (2016). Use of Biocomposite Adsorbents for the Removal of Methylene Blue Dye from Aqueous Solution. *American Journal of Materials Science,* 2016, 135-146. https://doi. org/10.5923/j. materials.20160605.03

[30] Munim, S. A., Saddique, M. T., Raza, Z. A., & Majeed, M. I. (2018). Preparation and physico-chemical characterization of β-cyclodextrin incorporated

chitosan biosorbent beads with potential environmental applications. *Materials Research Express,* 5(6), 065503. https:// doi: 10.1088/2053-1591/aac707

[31] Muttil, N., Jagadeesan, S., Chanda, A., Duke, M., & Singh, S. K. (2023). Production, types, and applications of activated carbon derived from waste tyres: an overview. *Applied Sciences,* 13(1), 257.

[32] Ngasotter, S., Xavier, K. A. M., Meitei, M. M., Waikhom, D., Madhulika, Pathak, J., & Singh, S. K. (2023). Crustacean shell waste derived chitin and chitin nanomaterials for application in agriculture, food, and health – A review. *Carbohydrate Polymer Technologies and Applications,* 6, 100349. https://doi.org/10.1016/j.carpta.2023.100349

[33] Qiu, Y., Hamilton, S. K., & Temenoff, J. (2011). Improving mechanical properties of injectable polymers and composites. In B. Vernon (Ed.), *Injectable Biomaterials* (pp. 61-91): Woodhead Publishing.

[34] Rodrigues, S. G. G., Lopes, G. S., Longhinotti, E., & Diógenes, I. Z. N. (2025). Chitosan pretreatment: evidence of enhanced mechanical stability and adsorption capacity to produce a hybrid material. *Journal of the Brazilian Chemical Society,* 36(5), 1-10.

[35] Rostami, M. S., & Khodaei, M. M. (2023). Chitosan-based composite films to remove cationic and anionic dyes simultaneously from aqueous solutions: Modeling and optimization using RSM. *International Journal of Biological Macromolecules,* 235, 123723. https://doi.org/10.1016/j.ijbiomac.2023.123723

[36] Rostami, M. S., & Khodaei, M. M. (2024). Recent advances in chitosan-based nanocomposites for adsorption and removal of heavy metal ions. *International Journal of Biological Macromolecules,* 270, 132386. https://doi.org/10.1016/j.ijbiomac.2024.132386

[37] Sanghi, R., & Bhattacharya, B. (2005). Comparative evaluation of natural polyelectrolytes psyllium and chitosan as coagulant aids for decolourization of dye solutions. *Water Quality Research Journal,* 40(1), 97- 101. https://doi.org/10.2166/wqrj.2005.009

[38] Sapuła, P., Bialik-Wąs, K., & Malarz, K. (2023). Are natural compounds a promising alternative to synthetic cross-linking agents in the preparation of hydrogels? *Pharmaceutics,* 15(1), 253.

[39] Thanasegaran, K., Yeap, S. P., Lai, L. S., & Wong, V. L. (2023). Chitosan powder vs. chitosan macrobead: feasibility test for separation of microalgae from real pond water. *Chemical Engineering Transactions,* 106, 1021-1026. https://doi.org/10.3303/CET23106171

[40] Thu, H. E., Haider, M., Khan, S., Sohail, M., & Hussain, Z. (2023). Nanotoxicity induced by nanomaterials: A review of factors affecting nanotoxicity and possible adaptations. *OpenNano,* 14, 100190. https://doi.org/10.1016/j.onano.2023.100190

[41] Upadhyay, A., Alimohammadi, F., & Tehrani, R. (2024). Engineering porosity-tuned chitosan beads: balancing porosity, kinetics, and mechanical integrity. *ACS Omega,* 9(31), 33857-33867.https://doi.org/10.1021/acsomega.4c03583

[42] Wong, V. L., Tay, S. Y., & Lim, S. S. (2020). Enhanced removal of methyl orange from aqueous solution by chitosan-CaCl2 beads. *IOP Conference Series: Materials Science and Engineering,* 736(2), 022049. https://doi.org/10.1088/1757-899x/736/2/022049

[43] Wu, L., Liu, X., Lv, G., Zhu, R., Tian, L., Liu, M., Liao, L. (2021). Study on the adsorption properties of methyl orange by natural one-dimensional nano-mineral materials with different structures. *Scientific Reports,* 11(1), 10640. https://doi.org/10.1038/s41598-021-90235-1

[44] Xiao, L., Shan, H., & Wu, Y. (2023). Chitosan cross-linked and grafted with epichlorohydrin and 2,4-dichlorobenzaldehyde as an efficient adsorbent for removal of Pb(II) ions from aqueous solution. *International Journal of Biological Macromolecules,* 247, 125503. https://doi.org/10.1016/j.ijbiomac.2023.125503

PROFILES

KABILARASAN THANASEGARAN completed his Master of Philosophy in Chemical Engineering at UCSI University in 2024. He obtained his Bachelor's degree from UCSI University, Malaysia. His research focuses on the synthesis of bio-adsorbents for applications in environmental remediation.
Email address: kabilarasan0527@gmail.com

SWEE PIN YEAP is currently an Associate Professor in the Department of Chemical and Petroleum Engineering at UCSI University. He obtained his PhD in Chemical Engineering in 2016 and has since made significant and sustained contributions to the field of nanoscience and nanotechnology. His research primarily focuses on the synthesis, functionalisation, and interfacial engineering of nanoparticles and low-dimensional nanomaterials for sustainable energy and environmental applications. He has established an independent research profile while actively contributing to postgraduate training and the broader scientific community.
Email address: yeapsw@ucsiuniversity.edu.my

LI SZE LAI is an Assistant Professor in the Department of Chemical and Petroleum Engineering, Faculty of Engineering, Technology and Built Environment, UCSI University, Malaysia. She holds a Doctor of Philosophy in Chemical Engineering and a Bachelor of Engineering (Honours) in Environmental Engineering. Her research interests focus on membrane technology for gas separation and wastewater treatment, including CO_2 capture, gas transport modelling, and the removal of heavy metals from wastewater. She also works on computational fluid dynamics (CFD) simulation, additive manufacturing, and the development of advanced membrane systems for environmental and industrial applications.
Email address: lails@ucsiuniversity.edu.my

JING LIN NG is a Senior Lecturer in the Faculty of Civil Engineering at Universiti Teknologi MARA (UiTM), Shah Alam, Selangor, Malaysia. She earned her PhD in Water Resources Engineering from Universiti Putra Malaysia (UPM) and her Bachelor of Engineering in Biological and Agricultural Engineering from the same university. Her research focuses on water resources engineering, hydrological modelling, climate change impacts, drought forecasting, artificial intelligence applications, and uncertainty assessment of hydrological models.
Email address: jinglin.ng@uitm.edu.my

CHAOMENG DAI is a Professor in College of Civil Engineering, State Key Laboratory of Disaster Reduction in Civil Engineering, Tongji University. His research focuses on groundwater security, including the migration and transformation of pollutants in groundwater, modeling and simulation of contaminant behavior, and the application of novel environmental functional materials/nanomaterials for groundwater remediation.
Email address: daichaomeng@tongji.edu.cn

KAH HON LEONG is an Associate Professor in the Department of Civil Engineering at University Tunku Abdul Rahman (UTAR). He holds a PhD in Civil and Environmental Engineering from University Malaya and professional qualifications from the Board of Engineers Malaysia and the Malaysia Board of Technologists. His research focuses on advanced material technologies for photocatalysis and environmental engineering applications. He is also an expert in ESG frameworks and green finance, specialising in sustainable investment strategies and ESG-linked industry practices.
Email address: khleong@utar.edu.my

PEY YI TOH is an Associate Professor in the Department of Petrochemical Engineering, Faculty of Engineering and Green Technology, Universiti Tunku Abdul Rahman. Dr. Toh obtained her Doctor of Philosophy in Chemical Engineering and Bachelor of Engineering (Hons) in Chemical Engineering, both from Universiti Sains Malaysia. Her research expertise focuses on magnetophoretic separation of microalgae, nanotechnology, environmental remediation, biofuel production, microalgal biosequestration, and phycoremediation, with an emphasis on developing sustainable solutions for environmental and energy applications.
Email address: tohpy@utar.edu.my